Stochastic Phase Switching of a Parametrically Driven Electron in a Penning Trap

L. J. Lapidus, D. Enzer, and G. Gabrielse
Department of Physics, Harvard University, Cambridge, Massachusetts 02138
(Received 7 January 1999)

Fluctuation-induced switching of driven bistable systems, far from equilibrium, has been the focus of theoretical analysis and analog circuit computations. A parametrically driven electron in a Penning trap is shown to be a nearly ideal experimental realization. Noise applied to this dynamic double well system produces random switching between two steady-state oscillations which differ in the oscillation phase by 180°.

PACS numbers: 05.40.Ca, 05.45.Ac, 05.70.Ln, 32.80.Pj

The study of fluctuation-induced switching between the two stable states of a bistable system began with Kramers's calculation of the rate of escape for a particle in a one dimensional double well potential [1], a system in equilibrium insofar as no probability currents are present in the steady state. Early experiments observed the switching between two modes [2] and two propagation directions [3] of a laser in equilibrium. Theoretical techniques have been extended to determine escape rates [4] and paths [5] for driven bistable systems which are far away from equilibrium in that divergence-less probability currents are present in the steady state. The only detailed experimental studies of such systems, however, have been analog computations done with circuits constructed to mimic the desired equation of motion [6,7].

In this Letter, experimental studies of a one-electron oscillator provide the first systematic study of switching in a driven, bistable physical system that is far from equilibrium. A single electron in a Penning trap is a nearly ideal realization of such a bistable oscillator when it is driven parametrically [8,9]. Noise induces switching between two steady-state oscillations which differ in their oscillation phase by 180°. The observed transitions are randomly spaced in time. The average transition rate depends upon the noise intensity, upon the strength and frequency of the parametric drive, and upon the adjustable nonlinearity of the oscillator. We compare to a recent theoretical model intended to describe our system [10].

The isolated electron oscillates about the center of a Penning trap [11]—a superposition of a $B = 3.6$ T magnetic field and a nearly ideal electrostatic quadrupole potential. The potential in this cylindrical Penning trap [12] arises from voltages applied to five copper electrodes [13], all of which are symmetric about an axis $\hat{z}$ in the direction of **B** (Fig. 1). The electrodes, and a completely surrounding vacuum enclosure, are cooled to 4.2 K by thermal contact to liquid helium, producing a vacuum measured to be better than 5×10^{-17} Torr in a similar apparatus [14]. The electron oscillator is thus not disturbed by collisions, observed earlier [15], which would prevent the observation of noise-induced switching.

Two of the three oscillatory motions of the trapped electron, both circular and perpendicular to the magnetic field, are neglected because their orbit sizes and kinetic energies can be kept negligibly small. The cyclotron motion at frequency $\nu_c' = 99.6$ GHz is damped to essentially its lowest quantum state by spontaneous emission. The radiation rate is enhanced by a resonant coupling to the TE_{115} radiation mode of the cylindrical trap cavity [16]. The magnetron orbit, at much lower frequency $\nu_m = 19$ kHz, is kept very small by sideband cooling [11].

The nearly harmonic axial oscillation along $\hat{z} \sim \mathbf{B}$ is the focus of this work. The oscillation frequency, $\omega_z/2\pi = 61.6$ MHz, depends upon the ratio of the electron's charge q and mass m, and upon the potential applied between the "end cap" and "ring" electrodes. Consider an electron on the trap axis, at a dimensionless location z from the center of the trap (measured in terms of a trap dimension $d = 0.354$ cm [11], so that $z \ll 1$). The electron moves along the axis under the influence of a restoring force $-m\omega_z^2 z[1 + \lambda_4 z^2 + \lambda_6 z^4]$, with the small "anharmonicity" terms proportional to λ_4 and λ_6 quantifying its nonlinearity. By varying the voltage applied to the two "compensation" electrodes, λ_4 can be tuned to $\lambda_4 = 0$, while λ_6 changes only slightly about the value $\lambda_6 \approx -0.27$. The axial oscillation induces an oscillating current I through a resonant LCR circuit. Power lost in the circuit (I^2R) weakly damps the oscillation at a rate

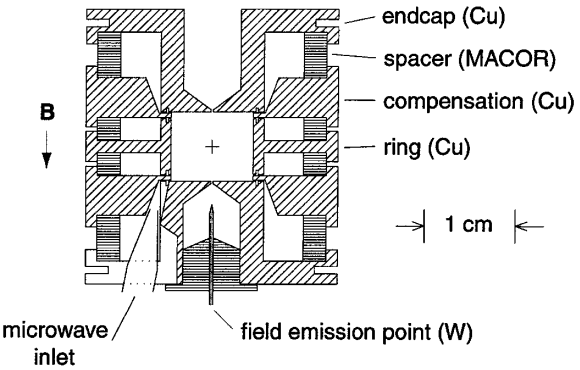

FIG. 1. Outline of the electrodes of the Penning trap. Gaps between electrodes are too small to be visible.

$\gamma_z = (10\ \mathrm{ms})^{-1}$. The induced voltage ($IR$) reveals the amplitude and phase of the axial oscillation.

The axial oscillation of the electron is driven parametrically by a strong coherent driving force near frequency $2\omega_z$, and also directly at frequencies near ω_z by weak fluctuating noise. The strong drive, $hm\omega_z^2 z\cos(\omega_d t)$, comes from modulating the trapping potential at nearly twice the resonant frequency of the oscillator, at $\omega_d = 2(\omega_z + \epsilon)$ with $\epsilon \ll \omega_z$. This parametric driving force excites a nearly resonant electron oscillation at half the drive frequency, $\omega_d/2 = \omega_z + \epsilon$, an example of the period doubling that occurs when a nonlinear oscillator is strongly driven.

The second drive is a fluctuating noise force mf_N applied to one end of the trap to directly and resonantly drive the electron's axial motion. Added electrical noise is "white" (i.e., frequency independent) over a 2 kHz bandwidth centered on ω_z, which is wider than all frequency widths relevant for the electron. As a confirmation, doubling the bandwidth of the applied noise does not change the rates of the transitions it induces. The applied noise power is parametrized later using the effective temperature T_N to which the resistor in the detection LCR circuit would need to be heated to produce Johnson noise of the same power per unit bandwidth. The relative power of radio frequency noise applied to a trap electrode can be accurately varied, but absolute measurements are more difficult. When the applied noise is removed, weak residual noise (perhaps from hard to measure trapping potential fluctuations that survive a 10 s RC low pass filter) continues to drive the oscillator.

The differential equation of motion for this driven axial electron oscillator is thus

$$\ddot{z} + \gamma_z\dot{z} + \omega_z^2[1 + h\cos\omega_d t]z + \lambda_4\omega_z^2 z^3 + \lambda_6\omega_z^2 z^5 = f_N\,. \qquad (1)$$

For small axial excitations, the nonlinear terms in Eq. (1) are negligible, and this equation reduces to the familiar, damped Mathieu equation [17] in the absence of noise (i.e., $f_N = 0$). The oscillation amplitude A grows exponentially when the strength of the parametric drive, (h), exceeds the threshold $h_T = 2\gamma_z/\omega_z$, provided that detuning of the parametric drive (ϵ) is within the excitation range $\epsilon_- < \epsilon < \epsilon_+$ where

$$\epsilon_\pm = \pm\frac{\omega_z}{4}\sqrt{h^2 - h_T^2}\,. \qquad (2)$$

Notice that for a drive strength well above threshold, ϵ_+ is a measure of the strength of the parametric drive.

The nonlinear terms in the differential equation grow rapidly as z grows. This arrests the exponential growth and results in a steady-state oscillation [9],

$$z(t) = A\cos[(\omega_z + \epsilon)t + \Psi]\,, \qquad (3)$$

$$\frac{5\lambda_6\omega_z}{16}A^4 + \frac{3\lambda_4\omega_z}{8}A^2 + \epsilon_+ - \epsilon = 0\,, \qquad (4)$$

$$\sin(2\Psi) = h_T/h\,. \qquad (5)$$

This solution of Eq. (1) (for $f_N = 0$, $\lambda_6 < 0$, and small λ_4) has a parabolic line shape for the square of the oscillation amplitude, A. Figure 2a shows the measured excitation range and amplitude, superimposed upon a parabolic line shape (dashed) for the parametrically driven electron oscillator when the drive frequency is increased during the measurement. We initially observe the same curve when sweeping the drive frequency downward. Once excited, however, the excitation persists even when the drive is swept downward in frequency into the range $\epsilon < \epsilon_-$. The expected hysteresis in this frequency range corresponds to the amplitude A taking either the value given by Eq. (4) or $A = 0$. The measured location of the resonance edge at drive detuning $\epsilon = \epsilon_+$ changed slowly during the many hours over which phase flips were measured for a fixed drive frequency and strength, because the trapping potential and hence ω_z were slowly drifting. Error bars on $\epsilon_+ - \epsilon$ include the drifts tolerated during measurements.

The bistability, or "double well," arises dynamically in this parametrically driven system because the phase Ψ, of the electron's steady-state oscillation, can have either of two values separated by 180°, as described by

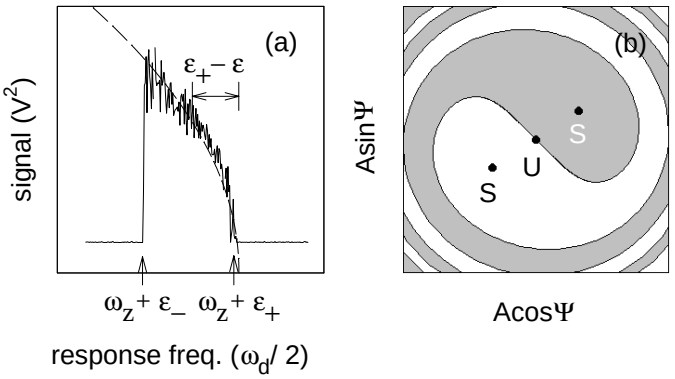

FIG. 2. (a) Observed parametric resonance of a single electron. (b) Phase space of a parametrically excited oscillator, with stable attractors labeled "S," and an unstable equilibrium labeled "U." The line traces the separatrix between two basins of attraction.

Eq. (5). Figure 2b shows the two steady-state attractors (labeled "S") within the phase space for this oscillator, for $\epsilon_- < \epsilon < \epsilon_+$ and $h > h_T$, in a reference frame rotating at $\omega_d/2$. Any transient excursion within the gray spiral eventually damps to the stable attractor within that spiral. Transient excursions within the white spiral similarly damp to its attractor. A novel feature is that these relaxations are very underdamped. The origin is an unstable solution ("U") for which there is no excitation amplitude and hence no uniquely determined oscillation phase.

Transitions between the two stable phases occur when noise fluctuations [i.e., $f_N \neq 0$ in Eq. (1)] carry the electron across the separatrix—the boundary between the gray and white regions in Fig. 2b. The measured phase of the electron's parametrically driven axial oscillation (Fig. 3a) then abruptly changes by 180° as the oscillator switches from one attractor to the other. The simultaneously measured amplitude (Fig. 3b), averaged with a 1 sec filter, shows that essentially every phase flip is accompanied by a collapse and regrowth of the oscillation amplitude. The most likely phase space trajectory between the attractors thus goes through or at least very near the unstable point U. This observation is consistent with the theoretical model [10].

The surprise here is that nearly every amplitude collapse (signifying that the system is near the unstable point U) is accompanied by a phase flip. We might expect that a phase flip would occur for only half of the amplitude collapses [10]. With no oscillation amplitude at point U, there is no defined oscillation phase. Following the oscillation collapse, we would then expect the parametrically driven oscillation to grow, with either oscillation phase being equally likely. Instead it seems that the amplitude collapse is rarely complete enough for the electron to lose

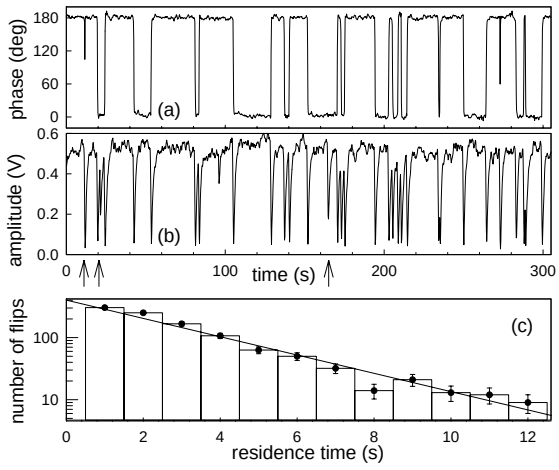

FIG. 3. Measured time series shows phase flips (a) and corresponding amplitude collapses (b) stimulated by residual noise, along with an exponentially decaying histogram of the time between phase flips (c). Three amplitude collapses, marked with arrows, lack a corresponding phase flip.

memory of its oscillation phase, and that the preferred trajectory in phase space goes past the unstable point rather than reversing in direction. An alternative explanation would be that amplitude collapses without phase flips are too short to be observed, but we know of no mechanism to cause such an asymmetry. This remarkable disagreement with the theoretical analysis begs for explanation. Perhaps an explanation can be found which is based upon the weak residual noise being less white than is assumed in the theoretical model.

Transitions between the two stable states of our double well are shown to be random insofar as a histogram of the time intervals between phase flips is an exponential (Fig. 3c). The average transition rate Γ can thus be determined from an exponential fit to the histogram, or equivalently by dividing a large number of observed flips by the time interval in which they occurred.

In Kramers's initial study of the rate of escape from a potential well [1,18], and in later extensions to systems driven away from equilibrium, the rate of escape from an attractor depends exponentially upon an activation energy E and a diffusion constant $D \sim T_N$ as $\Gamma \sim e^{-E/D}$. In the recent theoretical model [10], transitions induced by weak white noise take place via rare, large fluctuations which take the system from one attractor to the unstable equilibrium point U. The expected exponential dependence upon E/D implies that only the most probable path between an attractor and the unstable point will contribute to the probability of making a transition. A variational technique was used to identify this most likely path. For a strong parametric drive ($h \gg h_T$) and for nonlinearity parameter λ_4 tuned to $\lambda_4 = 0$, the theoretical analysis suggests that

$$\frac{E}{D} \sim \frac{1}{T_N} \frac{(\epsilon_+ - \epsilon)^a}{(\epsilon_+)^b}, \tag{6}$$

with exponents related by $b = a - 1/2$. For a parametric drive tuned near the upper edge of the excitation band, at $\epsilon \approx \epsilon_+$, the constants are $a = 3/2$ and $b = 1$. Unfortunately, the oscillation amplitude here is smaller than is required to reliably measure the oscillation phase. Away from the edge, fitting the author's numerical solution

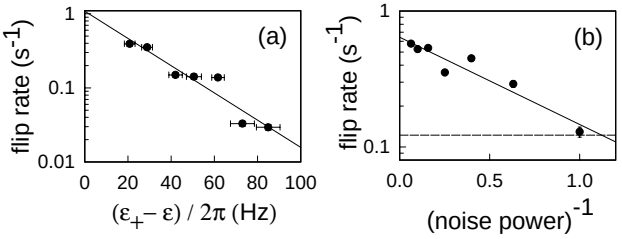

FIG. 4. (a) Rate of phase flips driven by residual noise versus detuning of a parametric drive with $\epsilon_+/2\pi = 100$ Hz. (b) The rate increases with added noise, as illustrated for detuning $(\epsilon_+ - \epsilon)/2\pi = 50$ Hz. The solid line is an exponential fit and the dashed line is the residual flip rate due to intrinsic noise.

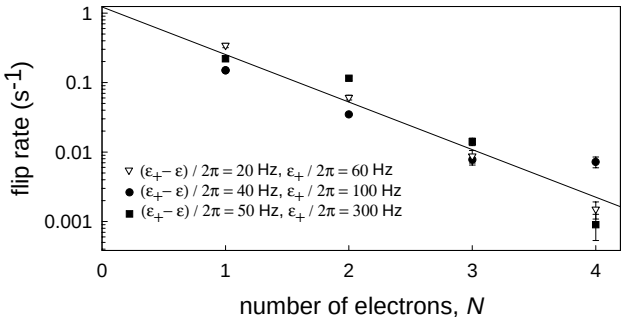

FIG. 5. Flip rates versus number of electrons for given detunings and strengths of the parametric drive.

yields $a = 1$ to within 10% over the range that we were able to access experimentally.

We looked experimentally to see if $\ln\Gamma \sim -E/D$ behaved as the predicted power laws in $\epsilon_+ - \epsilon$, in ϵ_+ and in T_N. Figure 4a and similar examples for different ϵ_+ (essentially different drive strengths) show that if we vary only the detuning from the upper edge of the resonance, $\epsilon_+ - \epsilon$, that $\ln\Gamma$ does go as a power law in this quantity when only residual noise is applied. A fit of such data to the form in Eq. (6) yields $a = 1.0 \pm 0.3$, and then $b = 0.8 \pm 0.4$, both consistent with the predictions. When we add noise power to increase the effective temperature T_N, Fig. 4b shows that the flip rate increases exponentially as predicted in Eq. (6). Unfortunately, the signal averaging used to see amplitude collapses makes it difficult to observe them when added noise increases their rate.

Finally, the measured flip rates for the center-of-mass motion of an N-electron oscillator with $N = 2$ through $N = 4$ depend on drive and noise in a similar way to that discussed for $N = 1$. The axial frequency ω_z is unchanged insofar as it depends on the ratio of the charge Nq and mass Nm, but the center-of-mass damping rate increases as $N\gamma_z$. The measured flip rates show that E/D varies in proportion to N, but not as $N\gamma_z$. For fixed detuning ϵ, drive strength (i.e., ϵ_+), and γ_z, Fig. 5 shows the flip rate decreasing exponentially with increasing N. When γ_z and N vary together, with $N\gamma_z$ remaining constant, E/D changes with N in the same linear way. Interestingly, when we slightly extend the one-electron model [10] to describe an N-electron oscillator, we obtain precisely this dependence. The neglected internal motions are apparently rendered unimportant due to sufficient cooling by internal collisional couplings and the resonant TE_{115} mode.

In summary, the parametrically driven one-electron oscillator is a nearly ideal realization of a double well system far from equilibrium. Measurements of the transitions and the crucial exponents illustrate that quantitative studies can be done on a well-controlled and well-characterized prototype system with a promising future. The comparison of our measurements with a theoretical analysis is a bit puzzling. On one hand, the theoretical model seems to be contradicted by experimental observations that an amplitude collapse nearly always results in a phase jump from one side of the double well to the other. On the other hand, the measured influence of damping and applied noise, along with measured crucial exponents, agrees with the theoretical predictions. Based upon what has been learned, the measurements could be significantly improved by reducing the fluctuations in the applied trapping potential. With better signal to noise, the nature of the collapse and revival of the excitation could be investigated in more detail. In future investigations, less cavity cooling of the cyclotron motion could easily be arranged, freeing trapped electrons to develop interesting and observable collective motions quite different from those described here. Similar apparatus and technique should thus make it possible to follow the onset of collective motions in a single component plasma as the number of electrons is increased from 1 to 10^6.

We are grateful for helpful conversations with M. Dykman and V. Smelyanskiy. A detailed preliminary report on this work is in the Ph.D. thesis of L. J. L. [19], and support came from the ONR and NSF.

[1] H. A. Kramers, Physica (Utrecht) **7**, 284 (1940).
[2] R. Roy, R. Short, J. Durnin, and L. Mandel, Phys. Rev. Lett. **45**, 1486 (1980).
[3] B. McNamara, K. Wiesenfeld, and R. Roy, Phys. Rev. Lett. **60**, 2626 (1988).
[4] M. I. Dykman and M. A. Krivoglaz, Sov. Phys. JETP **50**, 30 (1979).
[5] A. D. Ventsel' and M. I. Freidlin, Usp. Mat. Nauk. **25**, 5 (1970) [Russ. Math. Surv. **25**, 1 (1970)].
[6] D. G. Luchinsky and P. V. E. McClintock, Nature (London) **389**, 463 (1997).
[7] D. G. Luchinsky, P. V. E. McClintock, and M. I. Dykman, Rep. Prog. Phys. **51**, 889 (1998).
[8] C. Tseng and G. Gabrielse, Appl. Phys. B **60**, 95 (1995).
[9] C. H. Tseng, D. Enzer, G. Gabrielse, and F. L. Walls, Phys. Rev. A **59**, 2094 (1999).
[10] M. I. Dykman, C. M. Maloney, V. N. Smelyanskiy, and M. Silverstein, Phys. Rev. E **57**, 5202 (1998).
[11] L. Brown and G. Gabrielse, Rev. Mod. Phys. **58**, 233 (1986).
[12] G. Gabrielse and F. C. MacKintosh, Int. J. Mass Spectrom. Ion Phys. **57**, 1 (1984).
[13] J. Tan and G. Gabrielse, Appl. Phys. Lett. **55**, 2144 (1989).
[14] G. Gabrielse, X. Fei, L. Orozco, R. Tjoelker, J. Haas, H. Kalinowsky, T. Trainor, and W. Kells, Phys. Rev. Lett. **65**, 1317 (1990).
[15] D. Wineland, P. Ekstrom, and H. Dehmelt, Phys. Rev. Lett. **31**, 1279 (1973).
[16] J. Tan and G. Gabrielse, Phys. Rev. A **48**, 3105 (1993).
[17] M. Abramowitz and I. Stegun, *Handbook of Mathematical Functions* (Dover, New York, 1970), p. 722.
[18] H. Risken, *The Fokker-Planck Equation* (Springer-Verlag, New York, 1989), 2nd ed.
[19] L. J. Lapidus, Ph.D. thesis, Harvard University, 1998.